Intershell interaction in double walled carbon nanotubes: Charge transfer and orbital mixing

V. Zólyomi,[1,2] J. Koltai,[3] Á. Rusznyák,[3] J. Kürti,[3] Á. Gali,[4] F. Simon,[5] H. Kuzmany,[5] Á. Szabados,[2] and P. R. Surján[2]
[1]*Research Institute for Solid State Physics and Optics of the Hungarian Academy of Sciences, P.O. Box 49, H-1525 Budapest, Hungary*
[2]*Institute for Chemistry, Eötvös University, Pázmány Péter sétány 1/A, H-1117 Budapest, Hungary*
[3]*Department of Biological Physics, Eötvös University, Pázmány Péter sétány 1/A, H-1117 Budapest, Hungary*
[4]*Department of Atomic Physics, Budapest University of Technology and Economics, Budafoki út 8, H-1111 Budapest, Hungary*
[5]*Institut für Materialphysik, Universität Wien, Strudlhofgasse 4, A-1090 Wien, Austria*
(Received 2 October 2007; published 3 June 2008)

Recent nuclear-magnetic-resonance measurements on isotope engineered double walled carbon nanotubes (DWCNTs) surprisingly suggest a uniformly metallic character of all nanotubes, which can only be explained by the interaction between the layers. Here we study the intershell interaction in DWCNTs by density-functional theory and the intermolecular Hückel model. Both methods find charge transfer between the inner and outer tubes. We find that the charge transfer between the walls is on the order of 0.001 e^-/atom and that the inner tube is always negatively charged. We also observe orbital mixing between the states of the layers. We find that these two effects combined can in some cases lead to a semiconductor-to-metal transition of the double walled tube, but not necessarily in all cases. We extend our study to multiwalled nanotubes as well, with up to six layers in total. We find similar behavior as in the case of DWCNTs: electrons tend to be transferred from the outermost layer toward the innermost one. We find a notable peculiarity in the charge transfer when the (5,0) tube is present as the innermost tube; we attribute this to the σ-π mixing in such small diameter tubes.

DOI: 10.1103/PhysRevB.77.245403 PACS number(s): 73.22.−f, 71.15.Mb, 61.44.Fw

I. INTRODUCTION

Carbon nanotubes have been intensively studied in the past 15 years due to their high application potential and their rich physics. Single walled carbon nanotubes (SWCNTs), in particular, show fundamental phenomena ranging from, e.g., possible superconductivity[1] or Luttinger-liquid state[2,3] to Peierls distortion.[4] The electronic properties of SWCNTs are known to be fully determined by their (n,m) chiral indices (which essentially define the alignment of the hexagons on the SWCNT surface with respect to the tube axis).[5] Peapod annealing produced double walled carbon nanotubes (DWCNTs) (Ref. 6) also possess a number of unique properties such as very long phonon and optical excitation lifetimes.[7] DWCNTs are interacting systems consisting of two subsystems: an inner and an outer SWCNT. The subsystems are still well defined by their (n,m) chiral indices, but lose some of their identity due to the interaction, as suggested by recent experiments. Nuclear-magnetic-resonance (NMR) measurements show the extremely surprising result that the DWCNTs have a highly uniform metallic character.[8] This observation contradicts theoretical expectations for SWCNTs, especially in the diameter region of the inner tubes, where the curvature induces a secondary gap in nonarmchair tubes that should be metallic by simple zone folding approximation.[9] Therefore, these NMR observations can only be explained by the interaction between the inner and outer walls. The importance of the interaction is qualitatively easy to understand compared to the case of bundles, where the interaction surface of adjacent nanotubes is small; whereas in the case of double walled carbon nanotubes, the interaction surface between the two layers is 100%. Qualitatively, one expects charge transfer and/or orbital mixing to occur between the two walls due to the interaction.[10–16] Resonant Raman measurements have previously given experimental evidence for an orbital mixing related effect, the redshift of the Van Hove transition energies due to the interaction between the layers in DWCNTs, as well as for a dependence of the redshift on the intershell distance.[17] In addition, very recently, photoemission measurements have found evidence of charge transfer between the inner and outer layer of DWCNTs.[18,19]

In this work we present the results of our theoretical investigation of intershell interaction and its consequences in DWCNTs, as well as several multiwalled carbon nanotubes (MWCNTs). We studied 66 different DWCNTs by intermolecular Hückel (IMH) model.[20,21] We have also studied eight of these DWCNTs—three commensurate $(n,n)@(n',n')$, three commensurate $(n,0)@(n',0)$, and two commensurate $(n,m)@(2n,2m)$ DWCNTs—by first-principles density-functional theory (DFT) within the local-density approximation (LDA). We found a semiconductor-to-metal transition in two of the three $(n,0)@(n',0)$ DWCNTs studied by DFT, with only the third one retaining a small band gap. We have previously reported that our calculations predict a large density of states at the Fermi level in the case of metallic nonarmchair DWCNTs, and that starting from two semiconducting SWCNTs the resulting DWCNTs may transform into a metallic state, but not necessarily in every case.[22] In Ref. 22, we briefly outlined some of the results of the present paper, namely, that a small charge transfer (CT) from the outer wall to the inner wall occurs in every DWCNT. This effect has since been confirmed by photoemission spectroscopy.[18,19] Motivated by the experimental confirmation of our early results, we have further extended our calculations on charge transfer in DWCNTs, which we present in full detail in the following. We also find orbital mixing between the layers, which can explain the measured redshift of the resonance in the Raman measurements of DWCNTs.[17] We conclude that

the observed charge transfer and orbital mixing together can lead to a semiconductor-to-metal transition of DWCNTs, but not necessarily a near-universal metallicity.

We also extend our theoretical investigation to MWCNTs. We study up to six walled MWCNTs both with density-functional theory and the IMH model. We find that charge transfer in MWCNTs is very similar to that in DWCNTs, with electrons being transferred from the outermost wall to the inner walls. Based on the similarity between the interlayer charge transfers in MWCNTs and DWCNTs, we predict that similar shifts can be expected for the Van Hove peaks in the photoemission spectra of MWCNTs as in the case of the recently measured DWCNTs.[18,19] We find some peculiarities in the interlayer charge redistribution if the innermost tube has an extremely small diameter; we attribute this to the σ-π mixing appearing at such small diameters as a consequence of high curvature.[23]

II. METHOD

LDA calculations were performed both with a plane-wave [VASP (Ref. 24)] and a localized basis set [SIESTA (Ref. 25)] package. In the VASP calculations the projector augmented-wave method was applied using a 400 eV plane-wave cut-off energy, while in the SIESTA calculations double-ζ plus polarization function basis set was employed. For all achiral DWCNTs, 16 irreducible k points were used; comparison with test calculations using 31 k points showed this to be sufficient. For the chiral DWCNTs, less k points were used due to the size of the unit cells [five irreducible k points for (8,2)@(16,4) and one for (6,4)@(12,8)]. Likewise, we used only 5 irreducible k points in the calculations on MWCNTs (the largest MWCNT had 660 atoms in the unit cell). As these codes use periodic boundary conditions, only commensurate DWCNTs can be studied by them in practice. Otherwise, a model of incommensurate DWCNTs would require huge supercells. An alternate approach to compare the intershell interaction in different DWCNTs is the IMH model.[20,21] In this case the tight-binding molecular orbitals originate from the inner and outer tubes (orbital mixing). Using a Lennard–Jones-type expression to account for intercluster interactions, the tight-binding model has been applied to characterize weakly interacting carbon nanotubes.[26–29] The tight-binding principle can be generalized to apply to both intra- and intermolecular interactions,[30–32] leading to the IMH model,[20] which has been successfully applied to study DWCNTs (Ref. 21) and bundles of SWCNTs.[33] A detailed account of the model is given in Ref. 33. The IMH model allows us to calculate the CT for *any* DWCNT with good efficiency. Test calculations on the commensurate (7,0)@(16,0) DWCNT show that the infinite limit is easy to obtain from calculations on finite DWCNT pieces of gradually increasing length, and the error is less than 0.2%. Furthermore, optimizing the bond lengths by means of the Longuet–Higgins–Salem model[34,35] prior to the CT calculations, the charge transfer is altered by merely 0.8% as compared to the graphene wrapping model, showing that the CT is not very sensitive to the actual bond lengths at this level of theory.

III. DOUBLE WALLED TUBES

The DWCNTs considered in our calculations were selected based on Raman measurements.[17] The experimental diameter distribution of the outer wall of the DWCNTs was centered at 1.4 nm with a variance of 0.1 nm, while the ideal diameter difference between the inner and outer walls is 0.72 nm with a variance of 0.05 nm, corresponding to an inner diameter distribution centered at 0.68 nm. The Raman measurements clearly show that there is no chirality preference for the inner-outer tube pairs and a wide range of combinations can be found in the sample. In accordance with this, in the case of the IMH calculations we have chosen to examine the inner tubes which are at the center of the inner diameter distribution and to examine each inner tube with various outer tubes in order to examine the chirality dependence of the interactions. The diameter of each tube was taken from the usual graphene folding formulas with a uniform bond length of 1.41 Å; in the case of the LDA calculations, we used optimized geometries.[36] All inner tubes with diameters $d_{\text{inner}}=0.7\pm0.05$ nm were examined and for each inner tube; all outer tubes with diameters $d_{\text{outer}}=d_{\text{inner}}+0.72\pm0.04$ nm were considered, yielding a total of 60 different DWCNTs. In addition, we have also studied six other DWCNTs which are outside of the aforementioned diameter range, but could still be present in the sample, in order to compare with the LDA calculations. The eight commensurate DWCNTs studied by LDA were (4,4)@(9,9), (5,5)@(10,10), (6,6)@(11,11), (6,4)@(12,8), (7,0)@(16,0), (8,0)@(17,0), (9,0)@(18,0), and (8,2)@(16,4).

We calculated the band structure of the six commensurate achiral DWCNTs by both LDA packages and found fairly good agreement between localized-basis-set calculations and well-converged plane-wave results. The three armchair DWCNTs are all metallic, exactly as expected. Of the three zigzag DWCNTs, (8,0)@(17,0) remains a semiconductor, while the other two are metallic. Note that all zigzag SWCNTs considered were originally semiconducting: the LDA gaps of (7,0) and (16,0) were 0.21 and 0.54 eV, respectively (primary gaps), while those of (9,0) and (18,0) were 0.096 and 0.013 eV, respectively (curvature induced gaps).[9] The LDA band gap of (8,0)@(17,0) is about 0.2 eV, which is much smaller than that of the individual SWCNTs of about 0.6 eV.[9] The contraction of the gap in our calculations qualitatively agrees well with the findings of Song *et al.*[15] for the (7,0)@(15,0) and (8,0)@(16,0) DWCNTs. The band structures of the (7,0)@(16,0) and (8,0)@(17,0) DWCNTs are plotted in Figs. 1 and 2.

An earlier study of a linear carbon chain in SWCNT (Ref. 37) indicates that metallicity may occur due to charge transfer between the layers of the DWCNT. To investigate the reasons for metallicity in more detail, we have calculated the CT in the 66 DWCNTs in the IMH model. This is straightforwardly determined by summing up the contributions of the LCAO coefficients of every occupied molecular orbital separately for the atoms in the inner and outer walls and then comparing with the number of electrons that should be present on the given wall if there was no CT. Figure 3 shows our results for the charge transfer density (CT per unit length) along the tube axis as a function of the difference

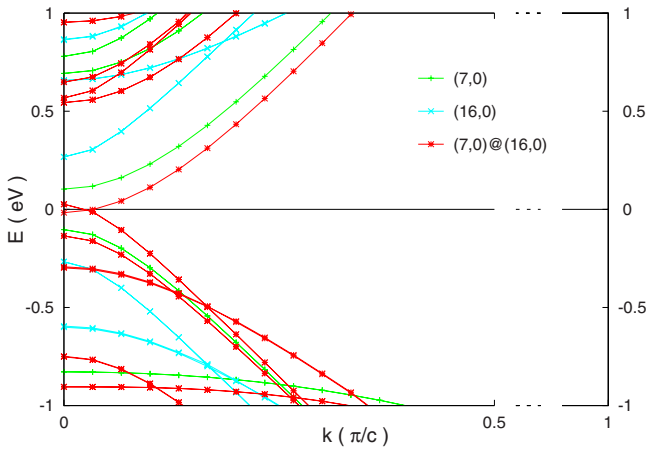

FIG. 1. (Color online) LDA band structure of the (7,0)@(16,0) DWCNT in comparison with the band structures of the subsystems in isolated single geometry (the Fermi levels are all shifted to 0 eV). c is the lattice constant of the nanotubes.

between the inner and outer diameters ($\Delta d = d_{\text{outer}} - d_{\text{inner}}$). In all cases, we found that the inner tubes are negatively charged. This result is in perfect agreement with recent observations of photoemission spectra of DWCNTs, which also predict negatively charged inner tubes.[18,19] Our calculated values for the CT density were between 0.005 and 0.035 $e^-/\text{Å}$. This corresponds to a range of about 0.0005–0.0045 e^-/atom for the inner wall and 0.0002–0.0024 e^-/atom for the outer wall; note that this CT is much smaller than what is typical in, e.g., alkali-intercalation experiments, but is still measurable by photoemission spectroscopy.[18,19] While the CT values show a decent amount of scattering, there is also a strong and clear overall decrease in the CT as Δd increases, which is expected, as the overlap between the orbitals of the two separate layers decreases as the distance between them increases. The large variance of the points is related to the difficulty of accurately

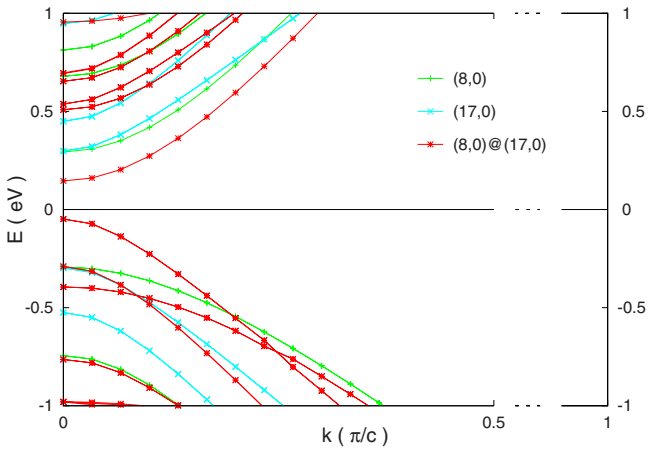

FIG. 2. (Color online) LDA band structure of the (8,0)@(17,0) DWCNT in comparison with the band structures of the subsystems in isolated single geometry (the Fermi levels are all shifted to 0 eV). c is the lattice constant of the nanotubes.

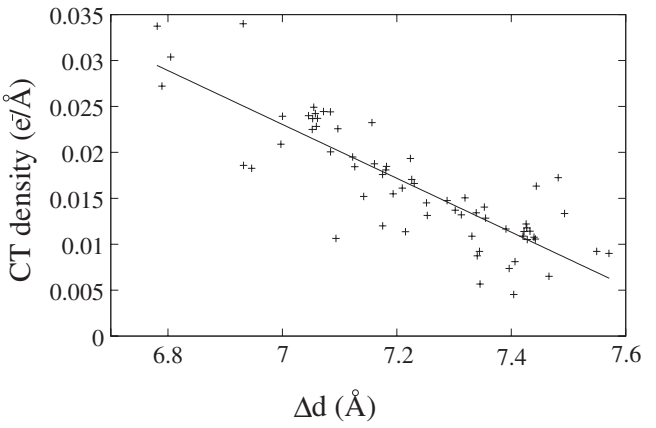

FIG. 3. Charge transfer density along the tube axis versus the diameter difference (Δd) between the inner and outer tubes of DWCNTs according to the IMH model (the inner tubes are always negatively charged). The straight line is a linear regression (see text).

predicting a CT of this order of magnitude. However, it is safe to conclude that the CT density in units of $e^-/\text{Å}$ can be estimated by the linear formula $-0.03\Delta d + 0.23$ with a considerable variance depending on tube chirality.

Advancing beyond the IMH model, we calculated the charge transfer for all eight commensurate DWCNTs by LDA. In the case of the plane-wave calculation, we were able to calculate Bader-type charges with Voronoi partitions (which define the borders of the atomic volumes by planes halfway between atoms, similar to the construction of Wigner–Seitz cells) using an external utility.[38] In the case of the localized-basis-set calculation, Mulliken population analysis could be performed. We found, that the direction and the order of magnitude of the CT are the same in these

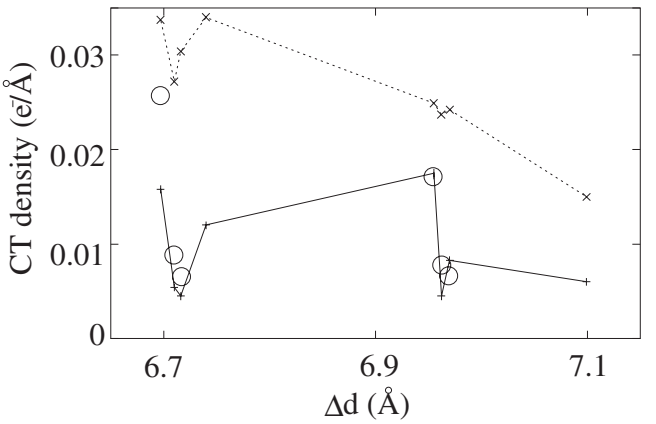

FIG. 4. Comparison between the IMH and LDA results for the charge transfer in DWCNTs. The CT values obtained from the VASP calculations by analyzing the Bader charges (solid) agree well with those obtained from the SIESTA calculations by Mulliken population analysis (circles), but both of them give a smaller value than the IMH method (dashed). The eight points of the VASP and IMH calculations correspond to (4,4)@(9,9), (5,5)@(10,10), (6,6)@(11,11), (6,4)@(12,8), (7,0)@(16,0), (8,0)@(17,0), (9,0)@(18,0), and (8,2)@(16,4) from left to right. For SIESTA, only the achiral DWCNTs are plotted (see text).

cases as what was found with the IMH model. The LDA CT is, however, somewhat smaller. This is illustrated in Fig. 4.

The Bader charges agree very well with the Mulliken charges for achiral DWCNTs. This is not necessary to occur, as the Mulliken population analysis usually performs well only in minimal basis set; however, if all atoms are of the same species (like in our case), then a larger basis set can also give reliable Mulliken charges and apparently such is the case in our calculations. However, in the case of the two chiral DWCNTs, the Mulliken population analysis yields a positively charged inner tube (not shown). In light of the good agreement between the Bader charges, the IMH analysis, and the photoemission measurements in Refs. 18 and 19, this is likely an erroneous result and can possibly be attributed to the basis-set-dependence problem of Mulliken charge analysis mentioned above. This result points out that when using a localized basis set, special care must be taken in the case of chiral tubes and most likely the basis set must be optimized further for these nanotubes.

The direction of this small charge transfer agrees with the Fermi levels as well. The small diameter inner tubes typically have a lower Fermi level than the larger diameter outer tubes. For example, according to our LDA calculations, the Fermi levels of (5,5) and (10,10) are −4.595 and −4.533 eV, respectively, and the Fermi levels of (8,0) and (17,0) are −5.045 and −4.774 eV, respectively. These results qualitatively agree with previous calculations in the literature.[16]

Based on the good agreement between the three different CT calculations, the Fermi level analysis, and the photoemission experiments cited earlier, we conclude that in DWCNTs electrons are transferred from the outer to the inner wall on the order of 0.005–0.035 e^-/Å, depending on tube chiralities.

IV. MULTIWALLED TUBES

In the following, we present our results on charge transfer between the layers of multiwalled carbon nanotubes, MWCNTs. We have calculated the interlayer charge transfer of altogether 15 different MWCNTs in a comparative study (1 six walled tube, 4 five walled tubes, 7 four walled tubes, 1 three walled tube, and 2 double walled tubes) both with LDA and the IMH model. We studied three series of MWCNTs, each with a standard ~3.4 Å layer separation between the adjacent layers of the multiwalled tube, with the exception of the (14,0)@(41,0) DWCNT, which was calculated in order to check whether any CT appears if there is no hybridization between the two layers. We studied the series starting with the (5,0), the (8,0), and the (12,0) tubes. Table I sums up our results. Each block of the table corresponds to one MWCNT, and CT values are written to a layer if it was present in the given geometry. The MWCNTs considered in the (5,0) series were the (5,0)@(14,0)@(23,0)@(32,0)@(41,0)@(50,0) six walled tube; the (5,0)@(14,0)@(23,0)@(32,0)@(41,0) and (14,0)@(23,0)@(32,0)@(41,0)@(50,0) five walled tubes; the (5,0)@(14,0)@(23,0)@(32,0), (14,0)@(23,0)@(32,0)@(41,0), and (23,0)@(32,0)@(41,0)@(50,0) four walled tubes; the (14,0)@(23,0)@(32,0) three walled tube; and the (23,0)@(32,0) and (14,0)@(41,0) double walled tubes [from left to right in Table I; (14,0)@(41,0) is not listed since the charge transfer is zero, exactly as expected due to the large interlayer distance, showing that CT only appears if the layers are close enough to interact]. In the (12,0) the following MWCNTs were considered: the (12,0)@(21,0)@(30,0)@(39,0)@(48,0) five walled tube and the (12,0)@(21,0)@(30,0)@(39,0) and (21,0)@(30,0)@(39,0)@(48,0) four walled tubes. Finally, in the (8,0) series, the (8,0)@(17,0)@(26,0)@(35,0)@(44,0) five walled tube and the (8,0)@(17,0)@(26,0)@(35,0) and (17,0)@(26,0)@(35,0)@(44,0) four walled tubes were studied.

As it can be seen in Table I, the results are very similar to what was found in DWCNTs: the IMH results in general give around twice as much charge per layer as the LDA, and the sign of the charges are generally identical in the two methods, with a generic trend of electrons being transferred from the outermost tube to the inner layers. In almost all cases, only the outermost layer loses electrons, while all other layers are negatively charged (albeit each MWCNT shows a different distribution of charges among the negative inner

TABLE I. Charge transfer between the layers of various multiwalled nanotubes. The upper half of the table lists the multiwalled tubes based on the (5,0) series, the left side of the lower half of the table lists the ones based on the (12,0) series, and the right side of the lower half of the table lists the ones based on the (8,0) series. (For the explanation of the columns, see text.)

IMH/LDA charge transfer (e^- per unit cell)								
(5,0)	0.105/0.175	0.105/0.168		0.105/0.174				
(14,0)	0.067/−0.046	0.067/−0.056	0.169/0.068	0.066/−0.040	0.169/0.068		0.169/0.053	
(23,0)	0.071/−0.021	0.070/0.002	0.074/0.016	0.050/−0.020	0.073/0.016	0.239/0.085	0.053/0.052	0.218/0.106
(32,0)	0.070/0.018	0.040/−0.002	0.071/0.038	−0.222/−0.114	0.040/0.032	0.075/0.035	−0.222/−0.105	−0.218/−0.106
(41,0)	0.026/0.015	−0.283/−0.111	0.026/0.022		−0.283/−0.116	0.026/0.021		
(50,0)	−0.340/−0.141		−0.340/−0.143			−0.340/−0.141		
(12,0)	0.022/0.042	0.022/0.042			(8,0)	0.125/0.026	0.125/0.026	
(21,0)	0.076/0.037	0.071/0.036	0.094/0.081		(17,0)	0.070/0.048	0.069/0.048	0.192/0.076
(30,0)	0.072/0.024	0.048/0.019	0.070/0.022		(26,0)	0.070/0.025	0.048/0.022	0.074/0.024
(39,0)	0.038/0.047	−0.142/−0.097	0.038/0.047		(35,0)	0.036/0.029	−0.243/−0.096	0.036/0.029
(48,0)	−0.208/−0.149		−0.208/−0.150		(44,0)	−0.302/−0.129		−0.302/−0.130

layers). The magnitude of the charge transfer onto each layer is also very similar: the IMH charges of the innermost tubes fall in the range of 0.0005–0.005 and 0.001–0.002 e^-/atom in the case of the outermost tubes. This striking similarity between the charge transfers found in MWCNTs and DWCNTs suggests that similar shifts can be expected in the Van Hove peaks in the photoemission spectra for MWCNTs as was recently found in the case of DWCNTs.[18,19] Since the outermost tube typically shows the largest magnitude for the CT (due to how it donates electrons to the inner layers), it is the outermost tube for which the Van Hove peaks in the photoemission spectrum will likely exhibit the largest shifts.

There is another interesting trend to be noticed in the case of multiple layers however, namely, some tube-specific trends for the charge per unit cell on each layer. For example, (30,0) and (26,0) have more or less the same charge value in all cases. The same trend can be seen for all other intermediate walls whenever there are at least four layers in total and the (5,0) tube is not present. This suggests that for intermediate walls within MWCNTs of four or more walls, the charge transfer values are well defined by the surrounding walls and are independent of the actual number of layers in the MWCNT. It is likewise interesting that if we take away the outermost (or the innermost) layer of an N-layer MWCNT, the charges on the innermost (or outermost) layer of the $(N-1)$-layer MWCNT do not change at all. For example, the charges of (8,0) are identical in the five walled (8,0)@(17,0)@(26,0)@(35,0)@(44,0) and the four walled (8,0)@(17,0)@(26,0)@(35,0). This result also suggests that the charges in MWCNTs are determined by the close environment; i.e., only the neighboring layers have an important effect on the charge of a given layer.

Note, however, that in the LDA calculations there are a few notable exceptions which do not fit in the generic trends mentioned above. All MWCNTs which include the (5,0) as the innermost tube show a somewhat different behavior in the LDA. The distribution of charges between the layers in the LDA calculations does not follow the generic trend: while the innermost tube always gains electrons, some intermediate layers are in fact positively charged (as opposed to other cases where only the outermost layer loses electrons), and the LDA and IMH results show distinct differences. This peculiar behavior suggests that the (5,0) nanotube has a strong electron affinity and may likely be caused by the σ-π mixing in the electronic structure of the small diameter (5,0) nanotube. We will return to this effect in the discussion below.

V. DISCUSSION

We found for the three commensurate $(n,0)@(n',0)$ DWCNTs that, due to the small magnitude of the charge transfer, the Fermi level is close to the Van Hove singularities that used to form the band gap of the single walled subsystems. This results in a large density of states at the Fermi level[22] (this can even be up to as high as an order of magnitude larger than the density of states at the Fermi level in armchair SWCNTs, depending on how close the Fermi level is to the peak of the Van Hove singularity which is shifted close to the Fermi level due to the interlayer interaction), similar to the case of chain@SWCNT systems.[37] Based on our IMH results, which say that the chirality dependence of the magnitude of the CT is more or less uniform, we can safely conclude that this large density of states at the Fermi level is expected in all nonarmchair metallic DWCNTs, as all nonarmchair single walled tubes have a band gap between two Van Hove singularities near the Fermi level at diameters above 0.5 nm.[9] Thus, we expect that the majority of the metallic DWCNTs have a large density of states at the Fermi level. This behavior is very similar to that of doped multiwalled tubes, which have previously been suggested as possible future superconductors.[1]

The case of the nonmetallic (8,0)@(17,0) DWCNT deserves attention. The two subsystems are semiconducting having almost the same band gap ($\approx$0.6 eV) at the LDA level.[9] The DWCNT they form remains semiconducting, but the bands near the Fermi level are distorted as compared to the rigid band prediction, such that the band gap drops to $\approx$0.2 eV. This result underlines the importance of orbital mixing and points out that the interaction between the inner and outer tubes is not limited merely to charge transfer, but the mixing of inner and outer tube orbitals is also an important part of the interaction. Furthermore, this result also shows that the orbital mixing caused by the intershell interaction provides the explanation to the experimentally observed redshift of the Van Hove transition energies.[17] The redshift is immediately understood by the contraction of the bands such as in the case of (8,0)@(17,0) in Fig. 2. In the experiments, all Van Hove transition energies show a redshift, with the lower energy transitions of a DWCNT suffering a greater shift than its higher energy transitions; our calculations show exactly the same qualitative trend. We mention that the experimental redshift is a few tens of meV, while our result for (8,0)@(17,0) is larger. This is due to that (8,0) has a smaller diameter than the center of the diameter distribution and is therefore not the most dominant example within the experimentally accessible inner tubes. In the case of (9,0)@(18,0) [(9,0) is at the very center of the diameter distribution], we find much smaller redshifts (roughly 0.02 eV for E_{11}), in agreement with experiments.

Thus, from the point of view of the electronic states, a DWCNT should—strictly speaking—always be considered as one single unified system. Approximating a DWCNT by separating it into an inner and an outer subsystem is of course possible, but it should always be done with caution. For example, if the orbital mixing were small, one could estimate whether a given SWCNT is likely to become metallic as one layer of a DWCNT by calculating the critical charge transfer (CT_{crit})—the CT at which the isolated tube becomes metallic upon doping—for the charged isolated SWCNT. However, this method is not reliable for DWCNTs because it completely neglects orbital mixing, which is obviously an important factor, as detailed above. In fact, we have calculated CT_{crit} for the two subsystems of the (8,0)@(17,0) DWCNT with this method and in both cases we obtained a value which is about a factor of 2 *smaller* than the CT from the DWCNT calculation. This contradictory result clearly shows that the question of whether a given DWCNT is metallic cannot be answered by means of calculating CT_{crit} on charged SWCNTs.

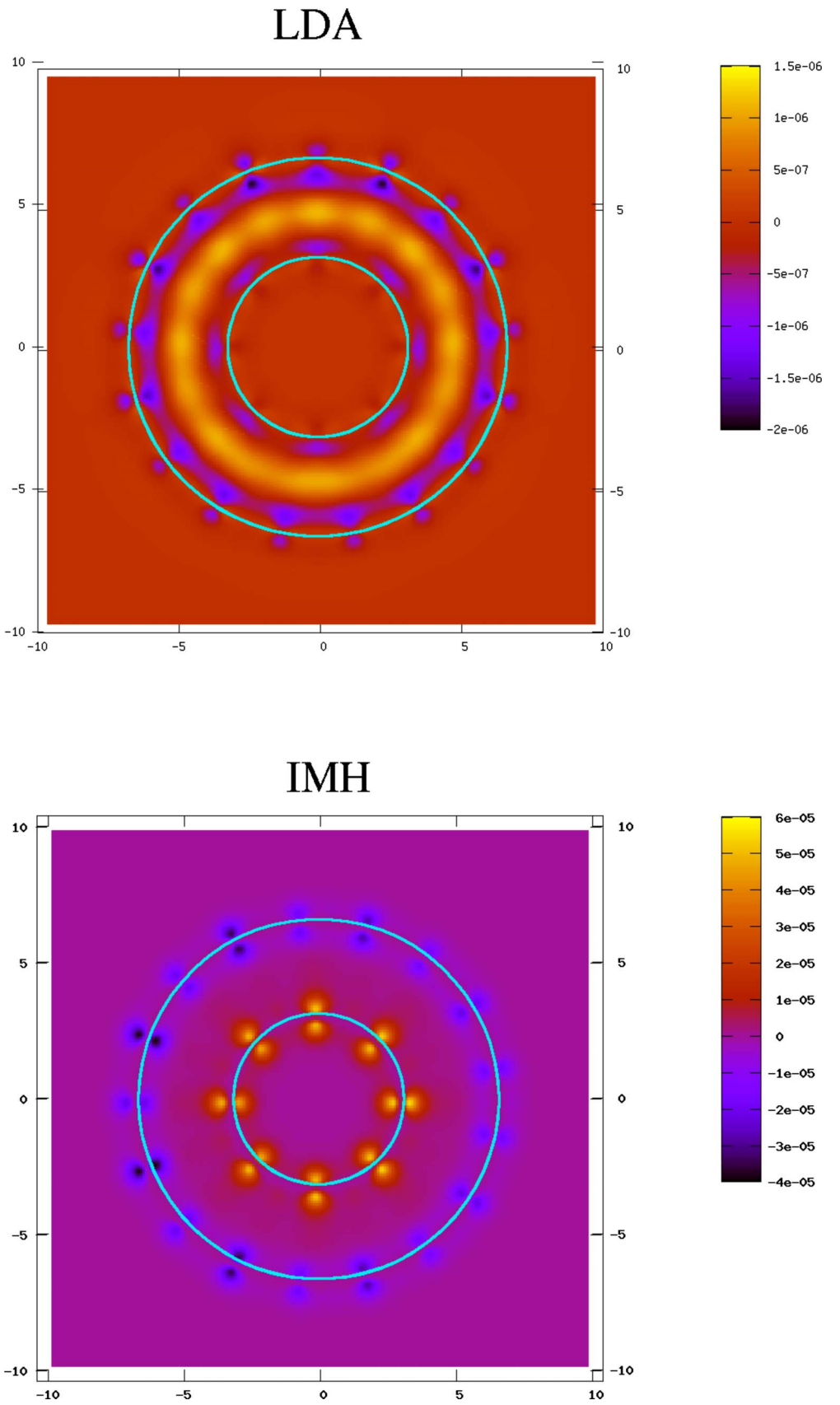

FIG. 5. (Color online) Charge redistribution profile (change of the electron density caused by interlayer interaction) in the case of the (8,0)@(17,0) DWCNT in one of the planes perpendicular to the tube axis containing the atoms (arbitrary units). The LDA results agree well with previous calculations (Ref. 16), while the IMH results show a more localized redistribution profile owing to the neglect of *s-p* mixing (see text).

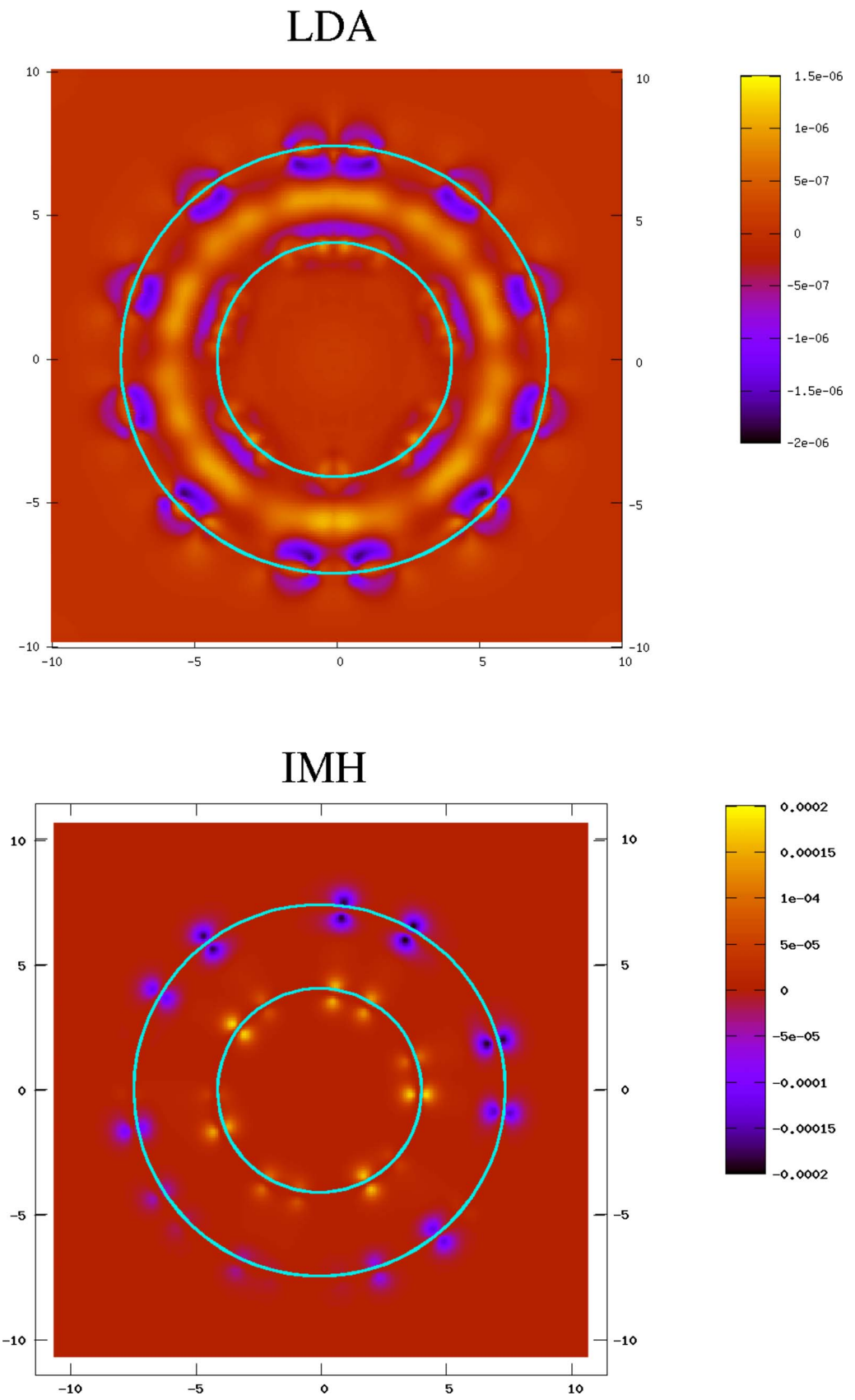

FIG. 6. (Color online) Charge redistribution profile (change of the electron density caused by interlayer interaction) in the case of the (6,6)@(11,11) DWCNT in one of the planes perpendicular to the tube axis containing the atoms (arbitrary units).

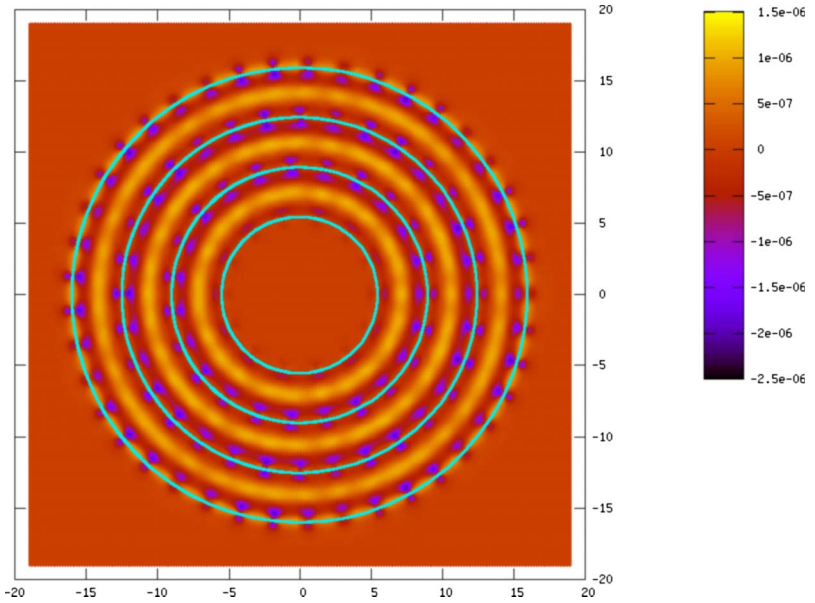

FIG. 7. (Color online) LDA charge redistribution profile (change of the electron density caused by interlayer interaction) in the case of the (14,0)@(23,0)@(32,0)@(41,0) MWCNT in one of the planes perpendicular to the tube axis containing the atoms (arbitrary units).

Another reason why it is not trivial to separate the two subsystems is the delocalized profile of the spatial distribution of the change of the electron density induced by the interlayer interaction which we will refer to as the charge redistribution profile. It has been pointed out in previous works in the local-density approximation that upon examining the contour plots of the change of the electron density in DWCNTs, it could be found that the electrons deplete from the walls and accumulate in the space between the layers.[12,13,16] We have also performed these calculations on the charge redistribution profile for the DWCNTs we examined and found good agreement with these previous works (see below). These results suggest that it is very difficult to divide the charges of the total charge density between the layers. Experiments, however, show that the layers behave more or less individually, as, e.g., Van Hove transitions of the inner and outer tubes can be clearly identified in Raman measurements.[17] Furthermore, recent measurements clearly identify an interlayer charge transfer in DWCNTs,[18,19] as mentioned earlier. We have used three different methods to calculate the charge transfer between the layers, and all three methods showed good agreement with the experimentally observed direction of the charge transfer. This shows that the charge transfer analyses we conducted are able to perform a plausible separation of the charge density between the inner and outer nanotubes.

In order to make a further comparison between the LDA and IMH results, we have calculated the charge redistribution profile using IMH as well. As mentioned above, the LDA results for the (8,0)@(17,0) are in good agreement with previous calculations.[16]

Our results are plotted in Figs. 5 and 6, showing the comparison between IMH and LDA in the case of the (8,0)@(17,0) and (6,6)@(11,11) DWCNTs. The IMH model shows a different redistribution profile from that of the LDA calculation, showing a picture in which the change is localized on the tube walls: the electrons deplete from the outer tube and accumulate on the inner wall (in accordance with our result on the direction of the CT). This result shows that, while it has great success at determining the CT between the layers, the IMH model fails to qualitatively reproduce the spatial charge redistribution profile which is seen in DFT calculations. The reason for this is possibly the neglect of *s*-*p* mixing. The IMH model relies on strictly *p*-type orbitals, thus neglecting the effect of charge depletion on the inside of a nanotube and charge accumulation on its outside due to the curved surface. This in turn leads to an insufficient description of the spatial charge distribution profile of the tubes, which could easily be the reason behind the observed differences in the charge redistribution profile. It is well known that curvature effects are important at diameters below 1 nm [and especially below 0.5 nm, as discussed below regarding the (5,0) tube]; hence, inclusion of *s*-*p* mixing is necessary to arrive at the correct spatial distribution of the charge density of DWCNTs. Finally, we mention that the charge redistribution profile apparently does not depend on metallicity, as the charge redistribution profiles of the semiconducting (8,0)@(17,0) qualitatively look the same as the charge redistribution profiles of the metallic (6,6)@(11,11) nanotube. The CT magnitudes are also largely independent of metallicity, as evidenced by Fig. 3.

Now returning to the multiwalled tubes, we present the LDA charge redistribution profiles of two MWCNTs, (14,0)@(23,0)@(32,0)@(41,0) in Fig. 7 and (5,0)@(14,0)@(23,0)@(32,0)@(41,0) in Fig. 8. The former figure shows a charge redistribution profile very similar to those found in double walled tubes. These are the typical charge redistribution profiles appearing in most MWCNTs we examined. However, as it can be seen in Fig. 8, the charge redistribution is strikingly different if the (5,0) tube is present as the innermost tube. In particular, there is a sharp peak exactly on the wall of the (5,0) tube, showing that the charges accumulate

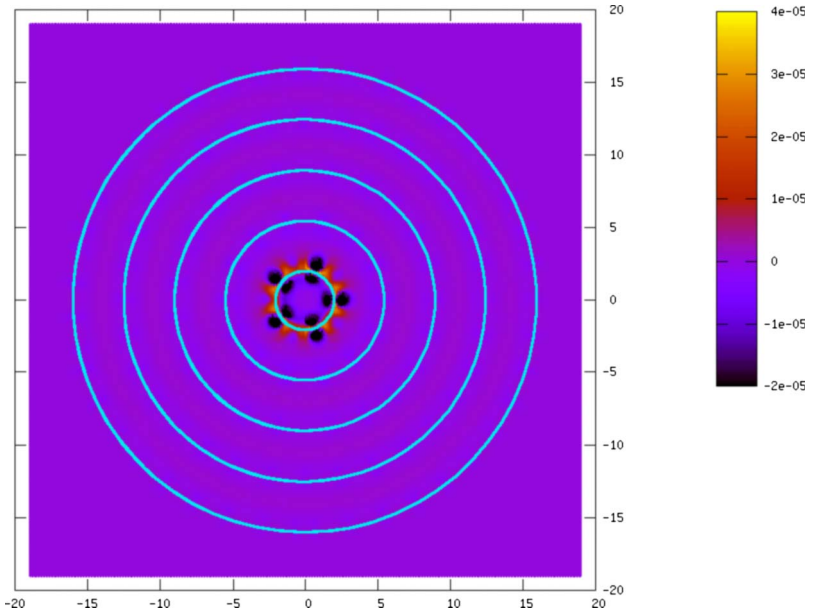

FIG. 8. (Color online) LDA charge redistribution profile (change of the electron density caused by interlayer interaction) in the case of the (5,0)@(14,0)@(23,0)@(32,0)@(41,0) MWCNT in one of the planes perpendicular to the tube axis containing the atoms (arbitrary units).

on the wall, as opposed to the usual cases where the charge accumulates in the interlayer region, suggesting that the (5,0) tube has a large electron affinity. This effect is caused by the very much different electronic structure of the (5,0) tube as opposed to the rest of the layers: (5,0) has a very small diameter of 4 Å, and at such small diameters, curvature induces a mixing between σ and π bands of the nanotube and a shift of bands, which in the end turn the (5,0) SWCNT into a metallic tube. The partially σ character of the bands crossing the Fermi level allows for slightly different interactions between the (5,0) and its neighboring layer, and this effect apparently cascades further onto the rest of the MWCNT, as it can be seen on the Bader charges of, e.g., (5,0)@(14,0)@(23,0)@(32,0)@(41,0)@(50,0), in the case of which the second and third innermost layers are positively charged. Note that the IMH charges in the MWCNTs containing the (5,0) tube do not show any peculiar behavior. This is precisely due to that *s-p* mixing is neglected in the IMH model. Thus, the striking difference between the IMH and Bader charges in the MWCNTs containing the (5,0) nanotube further expresses the importance of *s-p* mixing, especially in the case of extreme small diameters.

VI. CONCLUSIONS

In conclusion, we have performed calculations on a large number of double walled and multiwalled carbon nanotubes using density-functional theory and the intermolecular Hückel model. In the case of double walled tubes, we have found that electrons are transferred from the outer tube to the inner tube in all cases. We were able to quantify the charge transfer and found that the magnitude of the average charge transfer density along the tube axis ranges from 0.005 to 0.035 e^-/Å, depending on tube chiralities. We have found that interlayer orbital mixing is a very important part of the interaction between the layers and that the interactions can turn a DWCNT consisting of semiconducting subsystems into a metal, but not necessarily in every case. We predict that the majority of metallic DWCNTs have a high density of states at the Fermi level. We have also found that, although the CT values themselves agree within a factor of 2, the charge redistribution profile is qualitatively different in the IMH and the LDA calculations, possibly due to the neglect of *s-p* mixing in the former method. We have shown that interlayer charge transfer in multiwalled nanotubes is very similar to what can be seen in double walled tubes, with the outermost tube generally donating electrons to the inner layers. Based on this, we predict that for typical MWCNTs, similar shifts can be expected for the Van Hove peaks in the photoemission spectra as in the case of DWCNTs. We have also found that the charges of the layers of MWCNTs are determined by the close environment; i.e., only the neighboring layers have an important effect on the charge of a given layer. In the case of MWCNTs which contain the (5,0) nanotube as the innermost tube, we have shown that the charge redistribution between the layers is significantly different than in a general case, suggesting that the (5,0) tube has a large electron affinity and can likely be attributed to the strong σ-π mixing of the bands of the small diameter (5,0) tube.

ACKNOWLEDGMENTS

We thank O. Dubay and R. Pfeiffer for valuable discussions. Support from OTKA in Hungary (Grants No. F68852, No. K60576, No. T49718, No. NI67702, No. TS049881, No. F61733, and No. NK60984), the Austrian Science Foundation [Project No. I83-N20 (ESF-IMPRESS)], and the EU (Project No. MERG-CT-2005-022103) is gratefully acknowledged. F.S. acknowledges the Zoltán Magyary program, and V.Z. acknowledges the János Bolyai Research Scholarship of the Hungarian Academy of Sciences.

[1] L. X. Benedict, V. H. Crespi, S. G. Louie, and M. L. Cohen, Phys. Rev. B **52**, 14935 (1995).
[2] H. Ishii *et al.*, Nature (London) **426**, 540 (2003).
[3] B. Dóra, M. Gulácsi, F. Simon, and H. Kuzmany, Phys. Rev. Lett. **99**, 166402 (2007).
[4] D. Connétable, G. M. Rignanese, J. C. Charlier, and X. Blase, Phys. Rev. Lett. **94**, 015503 (2005).
[5] S. Reich, C. Thomsen, and J. Maultzsch, *Carbon Nanotubes* (Wiley, Berlin, 2004).
[6] S. Bandow, M. Takizawa, K. Hirahara, M. Yudasaka, and S. Iijima, Chem. Phys. Lett. **337**, 48 (2001).
[7] R. Pfeiffer, H. Kuzmany, C. Kramberger, C. Schaman, T. Pichler, H. Kataura, Y. Achiba, J. Kürti, and V. Zólyomi, Phys. Rev. Lett. **90**, 225501 (2003).
[8] P. M. Singer, P. Wzietek, H. Alloul, F. Simon, and H. Kuzmany, Phys. Rev. Lett. **95**, 236403 (2005).
[9] V. Zólyomi and J. Kürti, Phys. Rev. B **70**, 085403 (2004).
[10] D.-H. Kim, H.-S. Sim, and K. J. Chang, Phys. Rev. B **64**, 115409 (2001).
[11] D.-H. Kim and K. J. Chang, Phys. Rev. B **66**, 155402 (2002).
[12] Y. Miyamoto, S. Saito, and D. Tománek, Phys. Rev. B **65**, 041402(R) (2001).
[13] S. Okada and A. Oshiyama, Phys. Rev. Lett. **91**, 216801 (2003).
[14] Y. L. Mao, X. H. Yan, Y. Xiao, J. Xiang, Y. R. Yang, and H. L. Yu, Phys. Rev. B **71**, 033404 (2005).
[15] W. Song, M. Ni, L. Jing, Z. Gao, S. Nagase, D. Yu, H. Ye, and X. Zhang, Chem. Phys. Lett. **414**, 429 (2005).
[16] B. Shan and K. Cho, Phys. Rev. B **73**, 081401(R) (2006).
[17] R. Pfeiffer, F. Simon, H. Kuzmany, and V. N. Popov, Phys. Rev. B **72**, 161404(R) (2005).
[18] H. Shiozawa, T. Pichler, A. Grüneis, R. Pfeiffer, H. Kuzmany, Z. Liu, K. Suenaga, and H. Kataura, Adv. Mater. (Weinheim, Ger.) **20**, 1443 (2008).
[19] H. Shiozawa *et al.*, Phys. Rev. B **77**, 153402 (2008).
[20] A. Lázár, P. Surján, M. Paulsson, and S. Stafström, Int. J. Quantum Chem. **84**, 216 (2002).
[21] P. R. Surján, A. Lázár, and Á. Szabados, Phys. Rev. A **68**, 062503 (2003).
[22] V. Zólyomi, Á. Rusznyák, J. Kürti, Á. Gali, F. Simon, H. Kuzmany, Á. Szabados, and P. R. Surján, Phys. Status Solidi B **243**, 3476 (2006).
[23] X. Blase, L. X. Benedict, E. L. Shirley, and S. G. Louie, Phys. Rev. Lett. **72**, 1878 (1994).
[24] G. Kresse and J. Furthmüller, Phys. Rev. B **54**, 11169 (1996).
[25] P. Ordejón, E. Artacho, and J. M. Soler, Phys. Rev. B **53**, R10441 (1996).
[26] L. Henrard, E. Hernández, P. Bernier, and A. Rubio, Phys. Rev. B **60**, R8521 (1999).
[27] Y.-K. Kwon and D. Tománek, Phys. Rev. Lett. **84**, 1483 (2000).
[28] Y.-K. Kwon and D. Tománek, Phys. Rev. B **58**, R16001 (1998).
[29] A. Palser, Phys. Chem. Chem. Phys. **1**, 4459 (1999).
[30] S. Tabor and S. Stafstrom, J. Magn. Magn. Mater. **104**, 2099 (1992).
[31] S. Stafström, Phys. Rev. B **47**, 12437 (1993).
[32] M. Paulsson and S. Stafström, Phys. Rev. B **60**, 7939 (1999).
[33] Á. Szabados, L. P. Biró, and P. R. Surján, Phys. Rev. B **73**, 195404 (2006).
[34] H. C. Longuet-Higgins and L. Salem, Proc. R. Soc. London, Ser. A **251**, 172 (1959).
[35] M. Kertész and P. R. Surján, Solid State Commun. **39**, 611 (1981).
[36] J. Kürti, V. Zólyomi, M. Kertesz, and G. Sun, New J. Phys. **5**, 125 (2003).
[37] Á. Rusznyák, V. Zólyomi, J. Kürti, S. Yang, and M. Kertesz, Phys. Rev. B **72**, 155420 (2005).
[38] G. Henkelman, A. Arnaldsson, and H. Jónsson, Comput. Mater. Sci. **36**, 254 (2006).